

# Optical properties and aggregation of 1-N-methylamino-4'-nitroazobenzene in various environments

M. del P. Carreón-Castro<sup>a</sup>, M. Gutiérrez-Nava<sup>b</sup>, O.G. Morales-Saavedra<sup>c</sup>, J.M. Reyna-González<sup>b</sup>, and E. Rivera<sup>b,\*</sup>

<sup>a</sup> Instituto de Ciencias Nucleares, Universidad Nacional Autónoma de México,  
Circuito Exterior, Ciudad Universitaria, México, D.F. 04510, México.

<sup>b</sup> Instituto de Investigaciones en Materiales, Universidad Nacional Autónoma de México,  
Circuito Exterior, Ciudad Universitaria, México, D.F. 04510, México.

<sup>c</sup> Centro de Ciencias Aplicadas y Desarrollo Tecnológico, Universidad Nacional Autónoma de México,  
Circuito Exterior, Ciudad Universitaria, México, D.F. 04510, México.

Recibido el 4 de febrero de 2008; aceptado el 3 de abril de 2008

Aggregation of 1-N-methylamino-4'-nitroazobenzene (RED-H) was studied by UV-vis spectroscopy in solution, using different methanol: water mixtures as solvents, at different concentrations. In 100 % methanol, methanol: water 80:20 and 60:40, RED-H exhibited an maximum absorption wavelength at  $\lambda = 477$  nm and no aggregation was observed. By contrast, in mixtures of methanol: water 40:60 and 20:80 the appearance of an additional blue shifted band around  $\lambda = 430$  nm and a red shift of the absorption band to  $\lambda = 500$  nm followed by a long tail confirmed the presence of both H- and J-aggregates in these solvents. Theoretical estimations of aggregate stability carried out at the LMP2/aug-cc-PVTZ(-f)//MP2/6-31G level of theory showed that the H-aggregate is the more stable one (-14.9 kcal/mol) stabilized mostly by electronic correlation while the J-aggregate is much less stable, being stabilized by electrostatic interactions (-3.4 kcal/mol). Theoretical estimation of the absorption spectra of RED-H, H- and J-aggregates carried out using the TD-B3LYP method reproduces the experimentally observed spectra. All electronic transitions show a strong charge-transfer component.

**Keywords:** Aggregation; azo-dyes; DFT; LMP2; TD-DFT; optical properties.

Se estudió la agregación del 1-N-metilamino-4'-nitroazobenceno (RED-H) por espectroscopía UV-vis en solución, empleando como disolvente diferentes mezclas de metanol: agua a diferentes concentraciones. En metanol 100 %, y en mezclas metanol: agua 80:20 y 60:40, RED-H mostró una longitud de onda máxima de absorción a  $\lambda = 477$  nm y no se observó agregación. Por el contrario, en mezclas de metanol: agua 40:60 y 20:80, la aparición de una banda adicional desplazada hacia el azul alrededor de  $\lambda = 430$  nm, y el corrimiento hacia el rojo de la banda de absorción a  $\lambda = 500$  nm, seguida de una larga cola, confirmó la presencia de agregados H y J en estos disolventes. Las estimaciones teóricas de la estabilidad de los agregados, llevadas a cabo con un nivel de teoría LMP2/aug-cc-PVTZ(-f)//MP2/6-31G, mostraron que el agregado H es más estable (-14.9 kcal/mol), y es estabilizado, principalmente, por correlación electrónica, mientras que el agregado J es estabilizado por interacciones electrostáticas (-3.4 kcal/mol). La estimación teórica de los espectros de absorción de RED-H y de los agregados H y J, hecha con el método TD-B3LYP, reproduce los espectros observados experimentalmente. Todas las transiciones electrónicas muestran una fuerte componente de transferencia de carga.

**Descriptores:** Agregación; Azo-dyes; DFT; LMP2; TD-DFT; Propiedades ópticas.

PACS: 71.20..b; 71.20.Rv; 71.15.Mb

## 1. Introduction

Azobenzenes were initially used as dyes and have been widely studied for many research groups. Rau classified azobenzenes into three main groups based on their photochemical behavior [1]. Azobenzene itself belongs to the first category "azobenzenes" and could be considered a photochromic material because it has two isomers and exhibits two bands at  $\lambda = 313$  nm and  $\lambda = 436$  nm due to the  $\pi \rightarrow \pi^*$  and  $n \rightarrow \pi^*$  transitions, respectively [2]. The first band is more intense for the *trans* isomer and the second one for the *cis*. In addition, the latter possesses relatively poor  $\pi \rightarrow \pi^*$  and  $n \rightarrow \pi^*$  bands overlap. Substituted azobenzenes bearing electron-donor and electron-acceptor groups belong to the third category, "pseudostilbenes", and for this kind of azobenzenes  $\pi \rightarrow \pi^*$  and  $n \rightarrow \pi^*$  bands are inverted in the energy scale and become practically superimposed [1].

The incorporation of donor-acceptor substituted azobenzene units into polymers provide very versatile materials

from the application point of view due to the continuous reversible *trans-cis-trans* photoisomerization of the azobenzene groups and the photoinduced motions which occur when they are irradiated with laser polarized light [3]. The amino-nitro substituted azobenzene unit is the most commonly used. Recently, this research field has grown significantly and several reviews covering most of the implications of azobenzene photoisomerization in polymer structures have been published [4-8]. Natansohn *et al.* synthesized and characterized several azo-polymers bearing amino-nitro substituted azobenzene units, belonging to the pnMAN series (Fig. 1) [9-12]. In general, they exhibit maxima absorption wavelength around  $\lambda = 440 - 500$  nm, close to those reported for similar push-pull azo-compounds. Some azo-polymers have also been studied in Langmuir-Blodgett films and in these materials both J- and H-type aggregation have been observed [13-15].

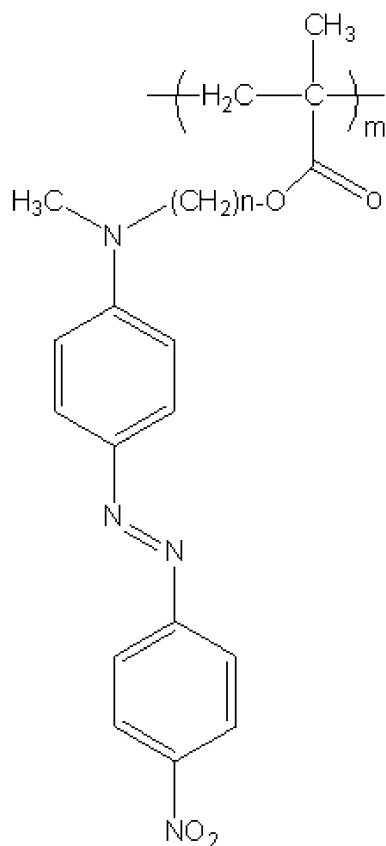


FIGURE 1. Structure of azo-polymers of the pnMAN series.

Since azo-polymers bearing amino-nitro substituted azobenzene units are highly versatile materials for optics and photonics, we have decided to carry out a study of the aggregation on the basic unit RED-H by absorption spectroscopy as a function of the polarity of the environment. Different methanol: water mixtures were used as solvents in order to study the solvatochromic effects. Increasing the polarity of the media gives rise to the formation of H-aggregates for this chromophore. To gain deeper insight into the nature of aggregation, a theoretical study has been carried out.

## 2. Experimental

### 2.1. Chemicals

1-N-methylamino-4'-nitroazobenzene (RED-H) was prepared according to the methods reported in the literature for the preparation of similar azo-compounds [16]. RED-H was dissolved in spectral quality solvents for UV-vis spectroscopy. Methanol, tetrahydrofuran (THF) and chloroform (spectrophotometric grade) were purchased from Aldrich. Prior to use, these solvents were checked for spurious absorption in the region of interest and found to be satisfactory. Absorption spectra of RED-H were recorded at room temperature on a UNICAM spectrophotometer (model UV-300) using 1cm quartz cells.

### 2.2. Computational details

The geometries of RED-H, H and J-aggregates were fully optimized at the MP2/6-31G level using the PC GAMESS version [Alex A. Granovsky, [www http://classic.chem.msu.su/gran/gamess/index.html](http://classic.chem.msu.su/gran/gamess/index.html)] of the GAMESS (US) QC package [17].

Head-to-tail configurations have been assumed for the dimers as most stable where the amino group is interacting with the nitro group of the adjacent molecule. Although the standard 6-31G basis set is too small for energy evaluation, it was shown that this level produces reasonably geometry in the case of naphthalene dimers [18]. To reach stabilization energies of H- and J-aggregates, local implementation of MP2 theory was used in combination with the cc-PVTZ basis set augmented with diffuse functions on the heavy atoms and removed f functions. This theoretical level is designated as LMP2/aug-cc-PVTZ. Single point energy evaluations were carried out with the Jaguar 5.0 program (Jaguar 5.0, Schrödinger, LLC, Portland, Oregon, 2002). Basis set superposition error has been corrected according to Boys *et al.* [19].

## 3. Results and discussion

1-N-methylamino-4'-nitroazobenzene (RED-H) (Fig. 2) was synthesized according to the methods reported in the literature by the reaction of protected N-methyl aniline in the presence of 4-nitro-benzenediazonium tetrafluoroborate at 0°C using acetic acid 50% as solvent, with further deprotection of the amino group. RED-H is an azo-dye that is totally soluble in many organic solvents such as chloroform, THF, methanol, ethanol, DMF and totally insoluble in water. Absorption spectra of RED-H were recorded in  $\text{CHCl}_3$ , THF and methanol and exhibited maximum absorption wavelength around  $\lambda = 470 \text{ nm}$  [20]. Absorption spectra were scanned at different concentrations in these solvents (from  $0.46 \times 10^{-5}$  to 0.001 M) and no aggregation was observed; the results are summarized in Table I.

TABLE I. Absorption data for RED-H in different solvents at a high concentration ( $2.5 \times 10^{-4} \text{ M}$ ) and in the solid state.

Solvent	$\lambda(\text{H-aggregates})$ [nm]	$\lambda_{\text{max}}$ [nm]	cut-off
chloroform	–	446	622
THF	–	458	625
methanol	–	464	630
methanol/water 80:20	–	476	650
methanol/water 60:40	421 (weak)	480	660
methanol/water 40:60	418	484	>800
methanol/water 20:80	412	488	>800
cast film ( $\text{CHCl}_3$ solution)	402	500	>800

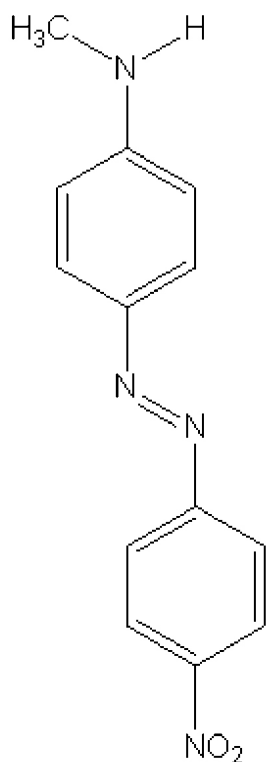
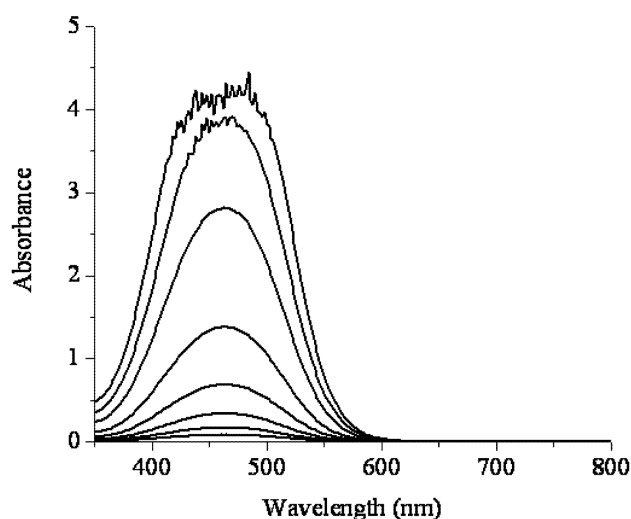


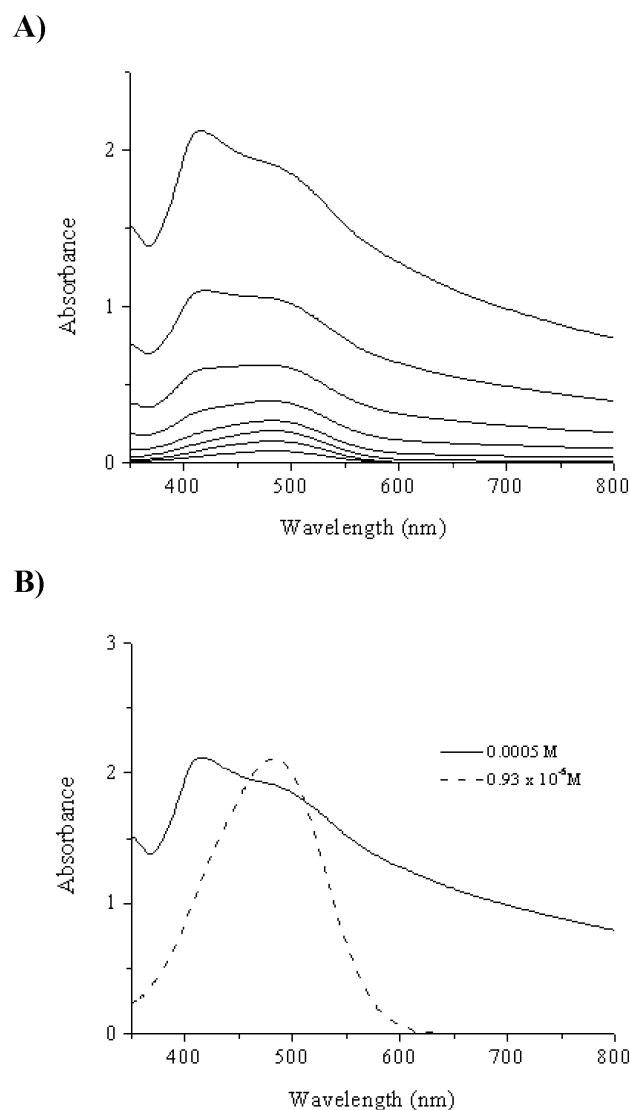
FIGURE 2. Structure of RED-H.

FIGURE 3. UV-vis spectra of RED-H in methanol at different concentrations. From top to bottom: a)  $2.5 \times 10^{-4}$  M, b)  $1.87 \times 10^{-4}$  M, c)  $1.25 \times 10^{-4}$  M, d)  $7.5 \times 10^{-5}$  M, e)  $3.75 \times 10^{-5}$  M, f)  $1.82 \times 10^{-5}$  M, g)  $0.93 \times 10^{-5}$  M, h)  $0.46 \times 10^{-5}$  M.

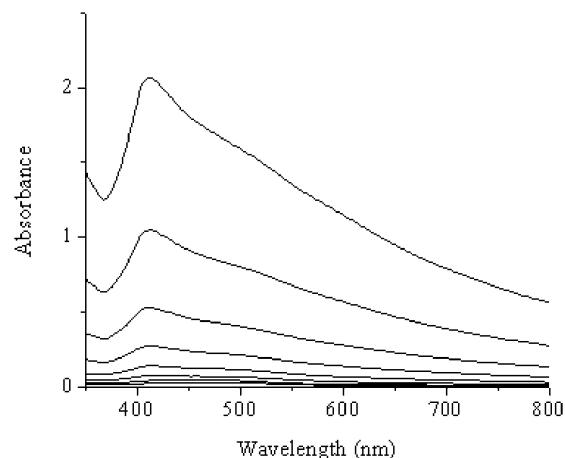
The azobenzene molecule is characterized spectroscopically by a low-intensity  $n \rightarrow \pi^*$  band in the visible region of the spectrum and a high-intensity  $\pi \rightarrow \pi^*$  band in the UV. Substitution by pull-push substituents like in 4-diethylamino-4'-nitro-azobenzene [21] increases the charge-transfer character (CT) of the  $\pi \rightarrow \pi^*$  transition along the long molecular axis and shifts the corresponding band far to the red, thus overlapping the weak  $n \rightarrow \pi^*$  band. The CT character of the

band causes a strong dependence of the band position on the solvent polarity [1].

UV-vis spectra of RED-H in methanol at different concentrations are shown in Fig. 3. This dye exhibited a maximum absorption wavelength at  $\lambda = 464$  nm with a cut-off at  $\lambda = 650$  nm. It has been verified that the Beer-Lambert law applies for diluted concentrations giving absorbances  $A \leq 3$ ; for this dye, no aggregation was observed in this particular solvent. RED-H behaved similarly in 80: 20 methanol: water mixtures, where  $\lambda_{\max}$  is only slightly red-shifted to 476 nm because of the polarity changes. Apparently, in methanol: water 60:40 ( $\lambda_{\max} = 480$  nm) traces of H-aggregation seemed to occur at high concentrations since the absorption band adopted an asymmetrical shape with a

FIGURE 4. UV-vis spectra of RED-H in methanol: water 40:60. **A)** at different concentrations. From top to bottom: a) 0.0005 M, b)  $2.5 \times 10^{-4}$  M, c)  $1.87 \times 10^{-4}$  M, d)  $1.25 \times 10^{-4}$  M, e)  $7.5 \times 10^{-5}$  M, f)  $3.75 \times 10^{-5}$  M, g)  $1.82 \times 10^{-5}$  M, h)  $0.93 \times 10^{-5}$  M, i)  $0.46 \times 10^{-5}$  M. **B)** at 0.0005 M and  $0.93 \times 10^{-5}$  M (normalized spectra).

A)



B)

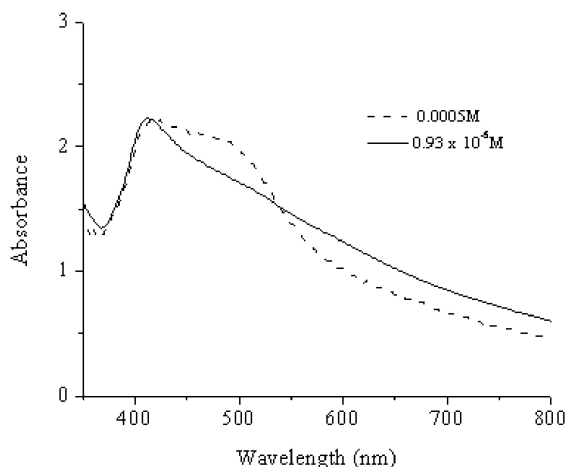


FIGURE 5. UV-vis spectra of RED-H in methanol: water 80:20. **A)** at different concentrations. From top to bottom: a)  $0.0005\text{ M}$ , b)  $2.5 \times 10^{-4}\text{ M}$ , c)  $1.87 \times 10^{-4}\text{ M}$ , d)  $1.25 \times 10^{-4}\text{ M}$ , e)  $7.5 \times 10^{-5}\text{ M}$ , f)  $3.75 \times 10^{-5}\text{ M}$ , g)  $1.82 \times 10^{-5}\text{ M}$ , h)  $0.93 \times 10^{-5}\text{ M}$ , i)  $0.46 \times 10^{-5}\text{ M}$ . **B)** at  $0.0005\text{ M}$  and  $0.93 \times 10^{-5}\text{ M}$  (normalized spectra).

relative inflexion around  $421\text{ nm}$ . However, when the UV-vis spectrum of RED-H at a dilute concentration ( $0.93 \times 10^{-5}\text{ M}$ ) was normalized and compared to that at a higher concentration ( $0.0005\text{ M}$ ) they proved to be practically identical. It is very well known that azo-polymers bearing amino-nitro substituted azobenzene units form H-aggregates in film in which the chromophores are paired in an antiparallel arrangement [22].

Absorption spectra of RED-H in methanol: water 40: 60 at a dilute concentration (Fig. 4a) displayed a maximum absorption wavelength at  $\lambda = 484\text{ nm}$  with a cut-off at  $\lambda = 650\text{ nm}$ . However, increasing concentration gives rise to an additional blue shifted band at  $\lambda = 418\text{ nm}$ , which reveals the formation of H-aggregates in this solvent. Moreover, the  $\lambda_{\text{max}}$  was red shifted to  $484\text{ nm}$  because of the CT character of this azobenzene unit. It is worth pointing out that RED-H

also showed a long tail in concentrated solutions with a cut-off exceeding  $800\text{ nm}$ ; this fact together with the red shift in  $\lambda_{\text{max}}$  revealed the existence of traces of J-aggregates.

In methanol: water 20: 80 (Fig. 5a), RED-H showed a maximum absorption wavelength at  $\lambda = 488\text{ nm}$ ,  $24\text{ nm}$  red shifted compared to that observed in methanol due also to the CT character of the molecule. In this system at a higher concentration, this dye exhibits an additional band at  $\lambda = 412\text{ nm}$ , which is proof of the presence of H-aggregates [20]. As in methanol: water 40: 60, RED-H showed a long tail with a cut-off beyond  $800\text{ nm}$  which provided evidence of the existence of traces of J-aggregates.

A comparison between absorption spectra at high and low concentrations in the last two systems has been carried out by normalizing the spectra at the dilute concentration. In methanol: water 40: 60 (Fig. 4b) there is no aggregation in the dilute solution; only an absorption band at  $\lambda_{\text{max}} = 484\text{ nm}$  is seen. Nevertheless, increasing the chromophore concentration gives rise to an additional absorption band at  $\lambda = 412\text{ nm}$ , which shows the existence of H-aggregates and a long tail due to the presence of some J-aggregates in this system. The cut-off beyond  $800\text{ nm}$  is an indication that a linear alignment of the molecules also takes place in solution. Therefore, in methanol: water 20: 80 (Fig. 5b) the absorption band is shifted to  $\lambda_{\text{max}} = 500\text{ nm}$  and one can also observe an additional aggregation band (H-aggregation) at  $\lambda = 412\text{ nm}$ [20]. In this particular solvent, aggregation takes place at low and high concentrations as shown in Figure 5b. Obviously the intensity ratio between H-aggregation band/monomer band is lower in dilute solutions.

Absorption spectrum of RED-H in casted film from a chloroform solution (Fig. 6) exhibited an maximum absorption wavelength at  $\lambda_{\text{max}} = 500\text{ nm}$ , red shifted with respect to that observed in chloroform solution ( $\lambda = 446\text{ nm}$ ), which is a clear proof of the existence of traces of J-aggregates in film. Moreover, an additional intense blue shifted absorption band is observed at  $\lambda = 402\text{ nm}$ , which is an indication of the presence of H-aggregates in the solid state. The intensity

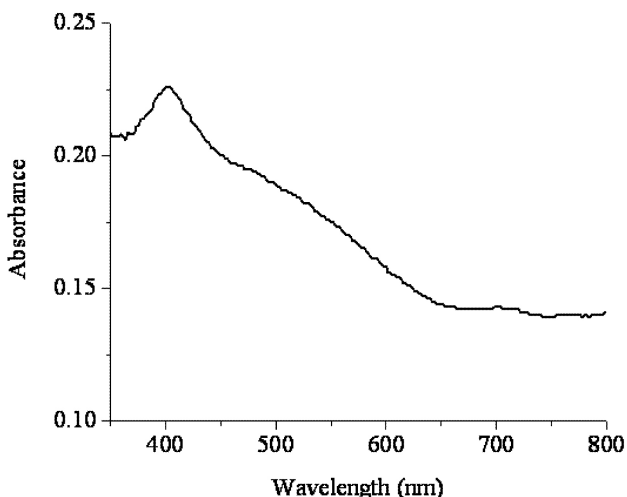


FIGURE 6. UV-vis spectra of RED-H in the solid state.

ratio  $A_{\text{complex}}/A_{\text{monomer}} \cong 1.12$  is slightly lower in film than in 40: 60 and 20: 80 methanol: water mixtures ( $A_{\text{complex}}/A_{\text{monomer}} \cong 1.23$ ). Thus, we can conclude that H-aggregation takes place predominantly in all the systems but in a higher proportion in solution than in film. Consequently, J-aggregation takes place more easily in film, since the molecules are better aligned in the solid state, as could be expected.

To get a deeper insight into the nature of intermolecular interactions in H- and J-aggregates, the theoretical study was performed. Figure 7 shows MP2/6-31G optimized geometries of H- and J-aggregates. As seen in the H-aggregate, RED-H molecules are bent so that they achieve better interaction between NHMe and NO<sub>2</sub> groups with distances between the N atoms of amino and nitro groups of 3.0 – 3.1 Å. The distances between benzene rings are somewhat large, 3.4 – 3.5 Å, characteristic of interplane distances in the parallel-displaced benzene dimer [23]. Table II shows stabilization energies of aggregates. As one can see, the H-aggregate is strongly destabilized at the SCF level while most of the stabilization energy comes from correlation stabilization, attaining almost 27 kcal/mol for the H-aggregate. This situation is very characteristic of aromatic dimers. Therefore, the H-aggregate is stabilized mainly by the interaction of  $\pi$ -electrons of the conjugated system of RED-H molecules. The destabilization at the SCF level for the H-aggregate is due to strong exchange repulsion [24].

Unlike the H-aggregate, where most stabilization energy comes from correlation energy, in the J-aggregate correlation energy contributes very little (only 0.6 kcal/mol) to overall stabilization energy, which reaches only -3.4 kcal/mol. It is worthy of note that SCF binding energy is negative for the J-aggregate and constitutes the main part of the stabilization energy. The overall geometry of the J-aggregate is more aligned (Fig. 7). The geometry of the J-aggregate prevents correlation stabilization by  $\pi - \pi$  interactions of aromatic units, therefore the stabilization of the J-aggregate is presumably

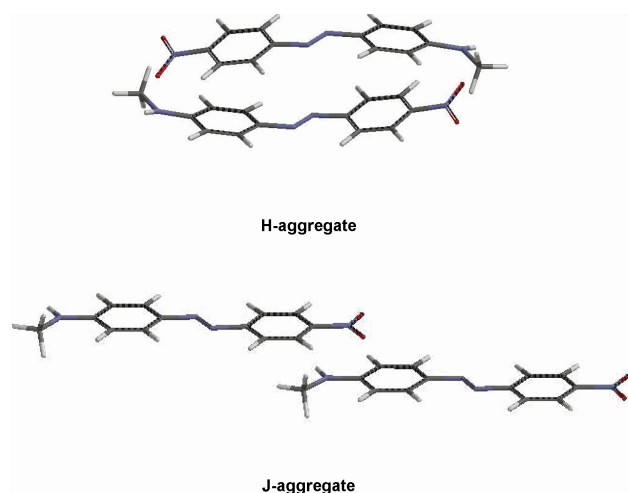


FIGURE 7. MP2/6-31G optimized geometry of RED-H, H- and J-aggregates.

TABLE II. BSSE corrected interaction energies of H- and J-aggregates at the LMP2/aug-cc-PVTZ(-f)//MP2/6-31G level (kcal/mol).

Complex	SCF <sup>a)</sup>	LMP2 <sup>b)</sup>	Ecorr <sup>c)</sup>
H-Aggregate	11.9	-14.9	-26.8
J-Aggregate	-2.8	-3.4	-0.6

a)BSSE corrected stabilization energies calculated at the SCF level

b)BSSE corrected stabilization energies calculated at the LMP2 level

c)Correlation stabilization calculated as the difference between LMP2 and SCF stabilization energies

TABLE III. Wavelengths ( $\lambda$ ) and oscillators strengths (f) of low lying transitions of RED-H, H- and J-aggregate calculated at the TD-B3LYP/6-31G\*/MP2/6-31G level of theory.

Compound	f <sup>a)</sup>	Coefficient <sup>b)</sup>	Excitation	$\lambda$ (nm)	
RED-H	0.75	0.64	HOMO-LUMO	466	
H-Aggregate	0.61	0.48	HOMO-1-LUMO	491	
			HOMO-LUMO+1		
			HOMO-LUMO+2		
		0.24	-0.23	HOMO-2-LUMO	434
			-0.22	HOMO-2-LUMO+2	
0.13	0.23	0.48	HOMO-LUMO+2		
		0.22	HOMO-3-LUMO	428	
		0.48	HOMO-2-LUMO		
J-Aggregate	1.51	0.53	HOMO-1-LUMO	495	
			0.37	HOMO-LUMO+1	

a)Transitions with oscillator strengths > 0.1

b)The largest coefficient; all other excitation coefficients are  $\leq 0.2$

due to electrostatic interactions of NO<sub>2</sub> and NHMe groups. No apparent NO<sub>2</sub>-HN hydrogen bonding has been detected in either of the two aggregates judging from the excessively long O-H distances (more than 2.5 and 3.5 Å in the H- and J-aggregate, respectively), which is in agreement with experimental data [25].

Table III shows the results of excited states modeling for RED-H and corresponding aggregates. As seen from Table III, time dependent B3LYP method reproduces long wave maximum absorption of RED-H. The HOMO-LUMO transition contributes most to the long wave maximum absorption, and excitation causes the charge transfer from the donor amino to the electron withdrawing nitro group as seen from Fig. 8.

H-aggregation produces a new blue shifted absorption band, which is located at  $\lambda = 400$ -430 nm depending on the solvent (Table 1). According to theoretical calculations the H-aggregate will have three important absorption bands in the visible region (Table III) at  $\lambda = 491$ ,  $\lambda = 434$  and  $\lambda = 428$  nm. From our point of view, the new transitions at  $\lambda = 434$

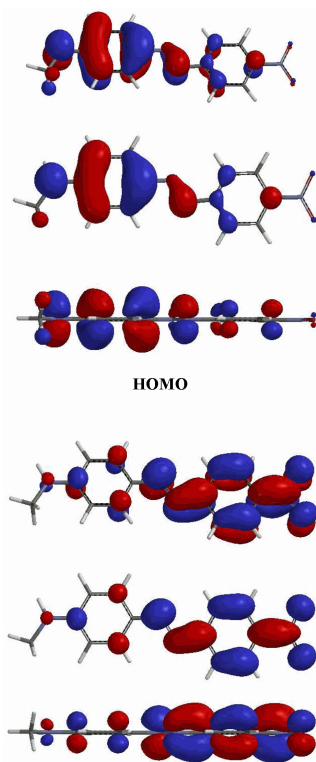


FIGURE 8. HOMO and LUMO molecular orbitals of RED-H (B3LYP/6-31G\*\*//MP2/6-31G level).

and  $\lambda = 428$  nm are responsible for the broad absorption band characteristic of H-aggregation observed in the range of  $\lambda = 400$ -430 nm. Table III shows that all these transitions are electron promotions from HOMO, HOMO-2 and HOMO-3 molecular orbitals to LUMO and LUMO+2 ones. Figure 9 shows the MO of H-aggregates contributing most to the corresponding transitions. As can be seen from Fig. 9, the transition at  $\lambda = 434$  nm represents symmetrical charge transfer from amino to nitro groups, while the transition at  $\lambda = 428$  nm is the charge transfer from azo to nitro groups. The long wave transition at  $\lambda = 491$  nm is similar to these or  $\lambda = 431$  nm and of monomer in terms of charge transfer and is definitely overlapped with the long wave absorption maximum from monomer RED-H.

Unlike the H-aggregate, the J-aggregate shows only one strong transition in the visible region close to  $\lambda = 500$  nm, which is in agreement with experimental data. This transition is the combination of HOMO-1-LUMO and HOMO-LUMO+1 excitations and represents a synchronic charge transfer from amino to nitro groups.

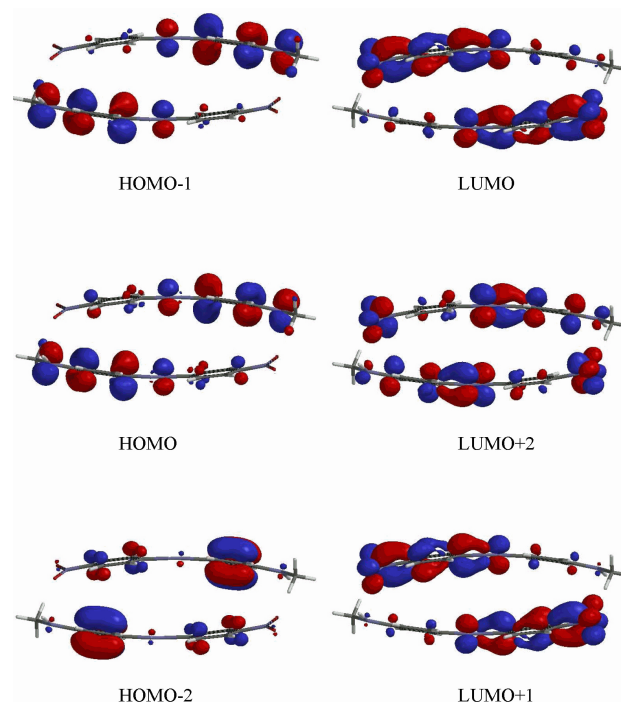


FIGURE 9. Most important molecular orbitals contributing to electronic transition in the visible region for the H-aggregate.

#### 4. Conclusion

The formation of both H- and traces of J-aggregates was observed for RED-H in highly polar environments (40: 60 and 20: 80 methanol: water solutions) as well as in the solid state. According to the band intensity ratio, H-aggregation takes place predominantly in all the systems; however the formation of J-aggregates for this dye is more favored in the solid state. Theoretical calculations show that the H-aggregate is the most stable one due to strong correlation stabilization, while the J-aggregate is stabilized primarily by electrostatic interactions of nitro and methylamino group. As follows from theoretical simulation of UV-vis absorption spectra of H- and J-aggregates, there is a strong charge transfer on excitation similar to that for long wave transition in monomeric RED-H.

#### Acknowledgements

We wish to thank PAPIIT-DGAPA for financial support (Projects IN-101207 and IN-102905). We also wish to thank Miguel Angel Canseco for his assistance in recording absorption spectra.

\* Author to whom correspondence should be addressed: e-mail: riverage@iim.unam.mx, Telephone: (5255)56 22 47 33, Fax: (5255) 56 16 12 10.

1. H. Rau, in *Photochemistry and Photophysics*, Rabek J.K., CRC Press (ed) (Boca raton: Florida, 1990) Vol.2, p. 119.
2. A. Natansohn and P. Rochon, *Can. J. Chem.* **79** (2001) 1093.

3. T. Todorov and L. Nikalova, *Appl. Opt.* **23** (1984) 4309.
4. S. Xie, A. Natansohn, and P. Rochon, *Chem. Mater.* **5** (1993) 403.
5. N.K. Viswanathan *et al.*, *J. Mater. Chem.* **9** (1999) 1941.
6. K. Ichimura, *Chem. Rev.* **100** (2000) 1847.
7. J.A. Delaire and K. Nakatani, *Chem. Rev.* **100** (2000) 1817.
8. A. Natansohn and P. Rochon, *Chem. Rev.* **102** (2002) 4139.
9. M.S. Ho, A. Natansohn, and P. Rochon, *Can. J. Chem.* **73** (1995) 1773.
10. X. Meng, A. Natansohn, P. Rochon, and C. Barrett, *Macromolecules* **29** (1996) 946.
11. A. Natansohn, S. Xie, and P. Rochon, *Macromolecules* **25** (1992) 5531.
12. S. Freiberg, F. Lagugné-Labarhet, P. Rochon, and A. Natansohn, *Macromolecules* **36** (2003) 2680.
13. A. Dhanabalan *et al.*, *Langmuir* **15** (1999) 4560.
14. D.S. Dos Santos *et al.*, *Polymer* **43** (2002) 4385.
15. D.S. Dos Santos *et al.*, *Synthetic Metals* **121** (2001) 1479.
16. E. Rivera, M. Belletête, A. Natansohn, and G. Durocher, *Can. J. Chem.* **81** (2003) 1076.
17. M.W. Schmidt *et al.*, *J. Comput. Chem.* **14** (1993) 1347.
18. C. Gonzalez and E.C. Lim, *J. Phys. Chem. A* **104** (2000) 2953.
19. S.F. Boys and F. Bernardi, *Mol. Phys.* **19** (1970) 553.
20. E. Rivera, M.P. Carreón-Castro, I. Buendía, and G. Cedillo, *Dyes and Pigments* **68** (2006) 217.
21. D.M. Shin, K.S. Schanze, and D.G. Whitten, *J. Am. Chem. Soc.* **111** (1989) 8494.
22. G. Iftime, F. Lagugné-Labarhet, A. Natansohn, and P. Rochon, *J. Am. Chem. Soc.* **122** (2000) 12646.
23. S. Tsuzuki, K. Honda, T. Uchamaru, M. Mikami, and K. Tanabe, *J. Am. Chem. Soc.* **124** (2002) 104.
24. S. Fomine, M. Tlenkopatchev, S. Martinez, and L. Fomina, *J. Phys. Chem. A* **106** (2002) 3941.
25. F. Lagugné-Labarhet *et al.*, *Macromolecules* **33** (2000) 6815.